Rotary ultrasonic machining of optical K9 glass using compressed air as coolant: a feasibility study

Chenglong Zhang, Weilong Cong, Pingfa Feng, Zhijian Pei

Rotary ultrasonic machining of optical K9 glass using compressed air as coolant:

a feasibility study

Abstract: Optical K9 glass has been used in a variety of applications, including optics, electronics, thermodynamics, and fluidics. It has been regarded as a difficult-to-cut material because of its superior mechanical properties. Rotary ultrasonic machining (RUM) using cutting fluid has been used successfully to machine many different types of brittle materials, such as ceramics, sapphire, and optical K9 glass. Dry machining has been successfully employed in the machining of some materials. However, there are no reported investigations on the RUM of optical K9 glass using compressed air as a coolant. This paper, for the first time, investigates the RUM of optical K9 glass using compressed air as a coolant. The experimental investigations focus on the effects of the input variables (ultrasonic power, spindle speed, and feedrate) on the output variables (edge chipping size, cutting force, surface roughness, and ultrasonic power consumption).

1. Introduction

Optical K9 glass is an outstanding functional material in many applications, including optics, electronics, thermodynamics, and fluidics. Because of its mechanical properties, such as high hardness, high strength, and low fracture toughness, it is regarded as a difficult-to-cut material. The machining of optical glass has attracted the attention of many researchers [1]. The current traditional machining methods used for optical glass include cutting, grinding, milling, and lapping. Fang and Chen have conducted experimental investigations of ultra-precision cutting for optical glass and explored the removal mechanism of brittle materials [2]. Belkhir et al. investigated the surface behavior during abrasive grain action in the glass lapping process and reported that the glass material removal rate during lapping depends on the cumulative actions of the individual grains [3]. Gu et al. presented a study on the horizontal surface grinding of optical glass BK7 using diamond grinding wheels and discussed the different material removal modes and the characteristics of the surface morphologies [4]. Arif et al. introduced the milling process into the ductile mode machining of optical glass and presented an analytical model to predict the critical feed per edge [5].

Some non-traditional machining processes have been applied to optical glass, such as abrasive water jet machining, electrolytic in-process dressing grinding, etc. Park et al.

conducted an experiment on the micro-grooving of glass using micro-abrasive jet machining [6]. They concluded that micro-abrasive jet machining could be effectively applied to the micro-machining of hard and brittle materials used for semiconductors, electronic devices, etc. Matsumura et al. applied abrasive water jet machining to micro machining and the fluid polishing of glass. A crack-free surface was finished using stagnation generated under the jet nozzle [7]. In addition, a study on the electrolytic in-process dressing grinding of optical glass showed that the electrolytic in-process dressing grinding could be an effective ultra-precision grinding process for hard and brittle materials [8].

Rotary ultrasonic machining (RUM), a non-traditional machining process, is a hybrid process that combines the material removal mechanisms of diamond grinding and ultrasonic machining [9]. The cutting tool is ultrasonically vibrated in the axial direction during processing, and the motion of the diamond particles on the diamond tool is a combination of rotation, ultrasonic vibration, and feeding. The machining process becomes milling if the feeding direction of the tool is perpendicular to the spindle axis and drilling if the feeding direction of the tool is parallel to the spindle axis; an illustration of the RUM process is shown in Fig. 1.
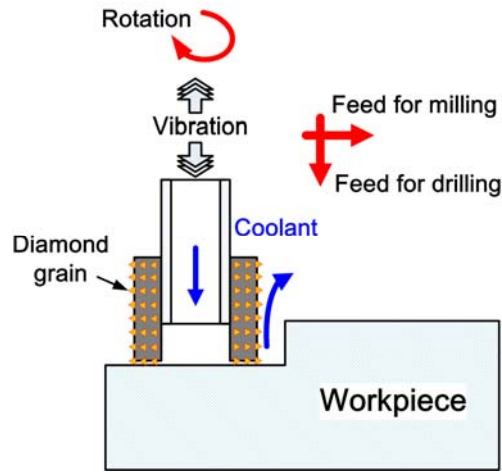
Fig. 1. An illustration of the RUM process [9].

Since RUM was developed in the 1960s, it has been used to machine many different types of brittle materials, such as ceramics, silicon, and glass. Pei et al. presented the modeling of the material removal rate in the RUM of ceramics [10], and Hu et al. studied the relationships between the material removal rate (MRR) and the controllable machining parameters based on the model [11]. They also stated that the RUM process can result in higher material removal rates than those obtained by diamond grinding. Li et al. reported a feasibility study on the RUM of ceramic matrix composites [12], and Cong et al. discussed edge-chipping in the RUM of silicon [13]. They showed that the RUM process can effectively reduce the edge chipping size. An investigation of the kinematic view of the tool life in the RUM of hard and brittle materials was conducted [14]. Furthermore, Zhang et al. studied the RUM of optical

glass. The literature review shows that compared with traditional machining processes, RUM has many advantages, including a smaller cutting force, a smaller edge chipping size, less subsurface damage, and less tool wear [15].

Using cutting fluids as coolants can improve the machinability of materials and enhance machining performance, which has been acknowledged since early in the 20th century [16]. A review showed that using cutting fluids as coolants in machining can reduce the friction and heat generated during the machining process, improve the quality of the machined surface and the tool life, and promote the removal of chips [17]. However, using cutting fluids as coolants in machining has resulted in some problems. First, the costs of cutting fluids, consisting of the deployment and disposal costs, account for approximately 10–20% of the manufacturing costs [18]. Second, cutting fluids containing chlorine, sulfur, and phosphorus have a great impact on the environment [19]. In addition, some cutting fluids are also hazardous to the operator's health.

The dry machining process was developed to reduce the problems caused by using cutting fluids as coolants. Studies have shown that dry machining using compressed air as a coolant can achieve satisfactory performance under certain machining conditions. Su et al. investigated the effects of cutting using compressed cooling air on tool wear, surface roughness and chip shape in the machining of difficult-to-cut materials. They showed that cooling air machining is not only environmentally friendly but also a great

improvement in the machinability of difficult-to-cut materials [20]. A feasibility study on the dry machining of Ti–6Al–4V alloy and the effects of cooling air temperature on machining performance was presented [21]. Nguyen and Zhang assessed the application of cold air and oil mist in surface grinding. They showed that using compressed air as a coolant can reduce the grinding force in the surface grinding of carbon steel [22]. However, there are few reports on using compressed air as a coolant in the RUM process. Cong et al. reported that the RUM of carbon fiber reinforced plastic (CFRP) using compressed cold air as a coolant is feasible under certain processing parameters [23]. A comparison between the RUM of CFRP using cutting fluid as a coolant and using compressed cold air as a coolant has been made [24].

There are many reported experimental investigations on the RUM of optical K9 glass using cutting fluids as coolants. Lv et al. presented surface observations and material removal mechanisms for the RUM of optical K9 glass. The authors also conducted a series of experimental studies on the RUM of optical K9 glass [25]. However, there is no report on the RUM of optical K9 glass without using cutting fluids as coolants. This paper, for the first time, presents an experimental study on the RUM of optical K9 glass using compressed air as a coolant. It reports the effects of the input variables (ultrasonic power, spindle speed, and feedrate) on the output variables (edge chipping size, cutting force, surface roughness, and ultrasonic power consumption). There are four sections in this paper. Following this introduction section is Section 2,

which describes the experimental conditions and measurement procedures. Section 3 shows and discusses the experimental results. Finally, the conclusions are summarized in Section 4.

2. Experimental conditions and measurement procedures

2.1 Experimental set-up

The experiments were conducted on a rotary ultrasonic machine (Series 10, Sonic-Mill, Albuquerque, NM, USA). Figure 2 shows the experimental set-up. It primarily consisted of an ultrasonic spindle system, cutting force and power consumption measurement systems, and a compressed air cooling system. The ultrasonic spindle system was comprised of an ultrasonic spindle, a power supply, and a control panel. The power supply converted conventional line voltage to 20 kHz of electrical energy. This high-frequency electrical energy was supplied to a piezoelectric converter that changed the high-frequency electrical energy to mechanical vibration. The ultrasonic vibration from the converter was amplified and transmitted to the cutting tool. This caused the cutting tool to vibrate at a frequency of 20 kHz. The amplitude of the ultrasonic vibration could be adjusted by changing the setting of the output control of the power supply. The vibration direction of cutting tool is axial during processing (shown in Fig. 2). A motor (SJ-PF, Mitsubishi Electric Corp., Tokyo, Japan) attached

atop the ultrasonic spindle supplied the rotational motion of the tool, and different speeds could be obtained by adjusting the motor speed controller.

The compressed air cooling system included an air compressor, a pressure regulator and valve, and a pressure gauge. The cooling system provided compressed air to the spindle and the interface of the machining.

There are two measurement systems: the cutting force measurement system and the ultrasonic power consumption measurement system. The cutting force measurement system consisted of a dynamometer, a charge amplifier, an A/D convertor, and a computer with software. The ultrasonic power consumption measurement system consisted of a current clamp, a voltage probe, a multimeter (Model 189, Fluke Crop., Everett, WA, USA), and a computer with the software Flukeview Forms (Version 3.4, Fluke Crop., Everett, WA, USA). The sampling rates of the current and the cutting force were set at 1 Hz and 100 Hz, respectively. More details about these two systems will be presented in Section 2.2.
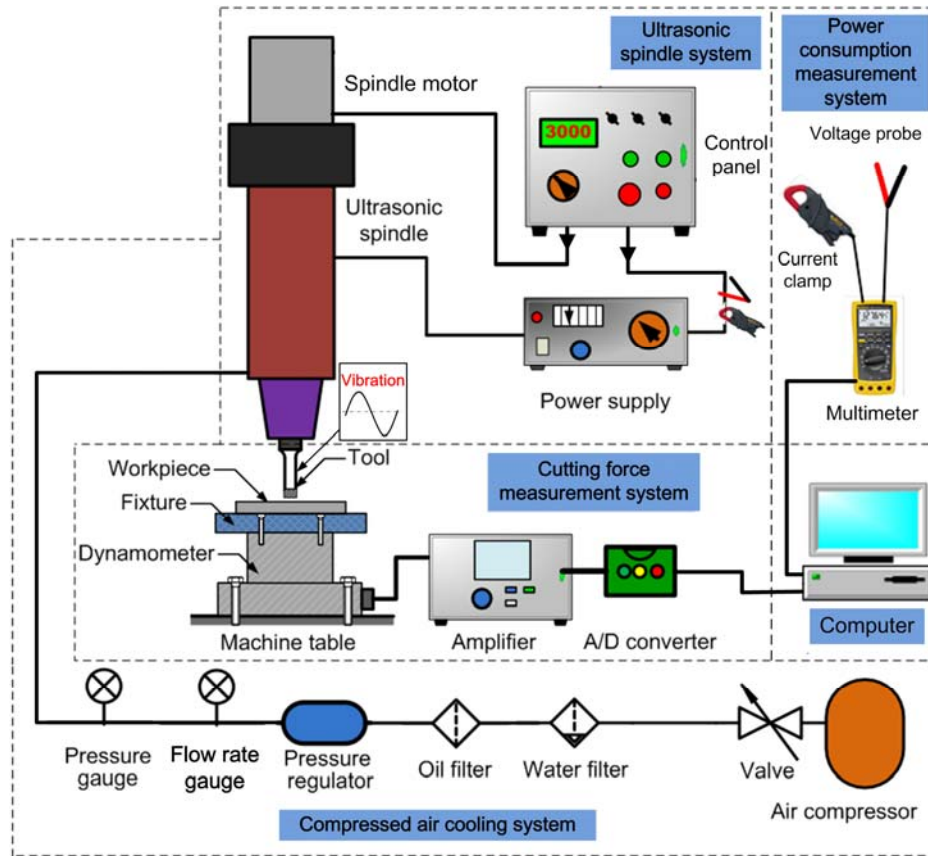
Fig. 2. Experimental set-up.

The workpiece was optical K9 glass with dimensions of 40 mm × 30 mm × 5 mm. The cutting tool was a metal-bonded diamond core drill with two slots (NBR Diamond Tool Corp., LaGrangeville, NY, USA). The outer and inner diameters (OD and ID) of the cutting tool were 9.54 mm and 7.34 mm, respectively, and the tuning length was 45 mm. The diamond abrasives had a mesh size of 180 and a concentration of 100. The metal bond was of the B type.

The experiments focused on studying the following input variables:

- Spindle speed: the rotational speed of the cutting tool;

- Feedrate: the feedrate of the cutting tool;

- Ultrasonic power: the percentage of power from the ultrasonic power supply controlling the ultrasonic vibration amplitude. Figure 3 illustrates the relationship between the ultrasonic power and the vibration amplitude. There is almost a linear relationship between the ultrasonic power and the ultrasonic vibration amplitude, and higher ultrasonic power will produce higher ultrasonic vibration amplitude [26].
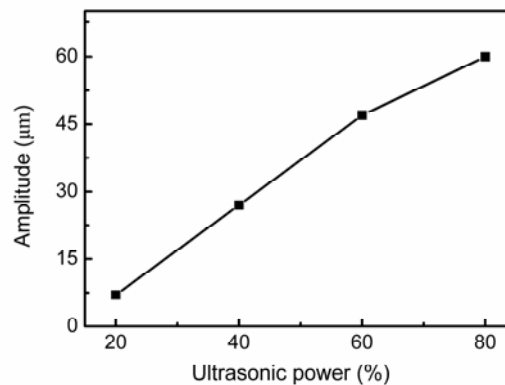

Fig. 3. Relationship between the ultrasonic power and the vibration amplitude.

The input variables and their values are listed in Table 1. Only one variable was changed at a time. The pressure and the flow rate of the compressed air were maintained at 30 psi and 1.5 lpm, respectively. Two holes were drilled under each machining condition.

Table 1. The input variables and their values

Variable	Unit	Value
Spindle speed	rpm	2000, 3000, 4000, 5000
Feedrate	mm/s	0.01, 0.02, 0.03, 0.04
Ultrasonic power	%	0, 20, 30, 40, 50

2.2 Measurement procedures for the output variables

A dynamometer (Model 9272, Kistler Inc., Switzerland) was used to measure the cutting force, and it was set on the machine table and beneath the workpiece. The electrical signals from the dynamometer were amplified by a charge amplifier (Model 5070A, Kistler Inc., Switzerland) and transformed into digital signals by an A/D converter. After being processed by a signal conditioner, the digital signals were saved on a computer by a data acquisition card (PC-CARD-DAS16/16, Measurement Computing Corporation, Norton, MA, USA) with the help of the software Dynoware (Type 2815A, Kistler Inc., Switzerland). The cutting force reported in this paper was the mean value of the cutting force in the axial direction of the tool during the RUM experiments.

The surface roughness was measured on the cylindrical surfaces of the machined holes. A surface profilometer (Surftest-402, Mitutoyo Corporation, Kanagawa, Japan)

was used with the tested range set at 1.6 mm. The surface roughness in this study was characterized by the average surface roughness (Ra). The roughness was measured at two locations along the axial direction of the hole: the entrance and the exit. At each location, two measurements were performed. Each measurement was repeated twice. The mean value of the measured Ra was used.

An optical microscope (BX51, Olympus America Inc., Melville, NY, USA) and a vernier caliper (model IP-67, Mitutoyo Corp. Kanagawa, Japan) were used to inspect and evaluate the edge quality on the exit side of each machined hole. The edge chipping size was chosen to evaluate the edge quality. Figure 4 shows the process of determining the chipping size. More details can be found in the literature [12].
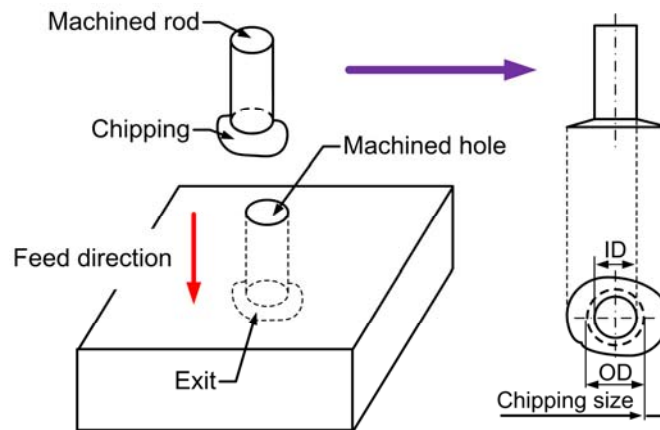

Fig. 4. Illustration of the edge chipping size.

The power consumption was the electricity energy (W) consumed by drilling 1 mm into the workpiece. It was calculated using

$$W_u = \frac{U_u \cdot I_u}{3600 \cdot F} \tag{1}$$

where W_u is the power consumption of the ultrasonic power supply (w·h/mm), U_u is the actual electrical voltage of the ultrasonic power supply (V), I_u is the measured current of the ultrasonic power supply during machining (A), and F is the feedrate (mm/s).

3. Experimental results and discussion

3.1 Edge quality

Figure 5 shows pictures of a machined hole and rod using RUM. Figure 6 presents the machining results of an optical K9 glass workpiece without ultrasonic vibration (called diamond drilling below), where Fig. 6(a) is the picture of the machined hole and Fig. 6(b) is the cutting force curve during the machining process. The hole cannot be drilled successfully using compressed air as coolant when the ultrasonic power is at 0%. Fig. 5(A) and (B) show that edge chipping at the entrance of the hole is better than that produced at the exit of the hole. Fig. 5(c) shows the machined rod during the processing since the used diamond tool is a hollow drilling tool.
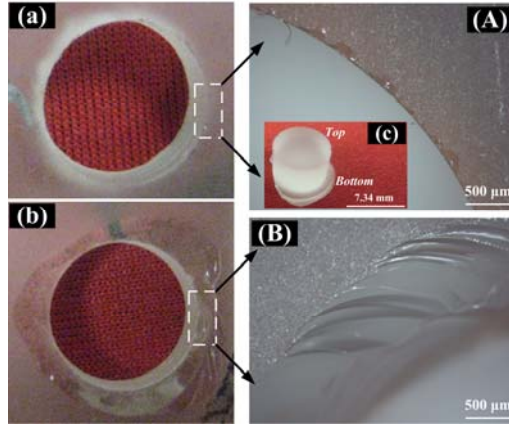
Fig. 5. Pictures of the machined hole and rod: (a) entrance, (b) exit, (c) machined rod, (A) a magnified view of the entrance marked in (a), (B) a magnified view of the exit marked in (b). (Ultrasonic power = 30%, spindle speed = 3000 rpm, and feedrate = 0.02 mm/s.)

Two stages of the cutting force curve are induced in the diamond drilling, as shown in Fig. 6(b). The cutting force of the first stage is relatively stable, which means that this stage is an effective machining process and the stage at which the machined region is produced (see Fig. 6(a)). The cutting force shows a strong fluctuation in the second stage, which means that serious cracks are induced, and the brittle fracture of the workpiece is generated during this stage (see Fig. 6(a)), which results in damage to the workpiece and failure to produce a hole.
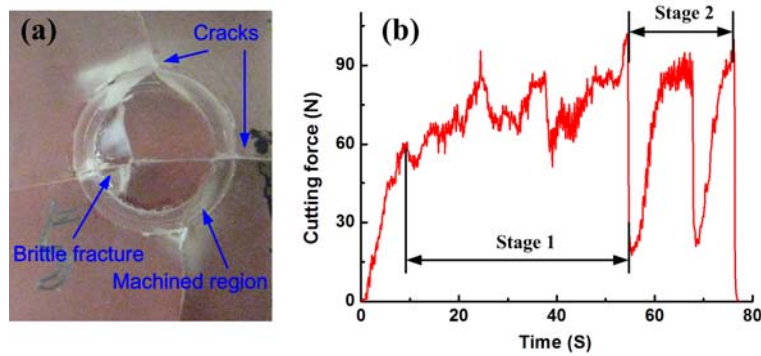
Fig. 6. Machining results without ultrasonic vibration: (a) machined hole, (b) cutting force curve. (Ultrasonic power = 0%, spindle speed = 3000 rpm, and feedrate = 0.02 mm/s.)

In drilling hard-brittle materials (such as ceramics, glass, etc.), edge chippings (chipping thickness and chipping size) are important criteria to evaluate the hole quality because they influence the component quality or the positioning accuracy during assembly. Figure 7 shows the effects of the ultrasonic power, spindle speed, and feedrate on the edge chipping size. The figure also shows that the change of the edge chipping size is not monotonic with an increase in the ultrasonic power. The chipping size decreases slightly when the ultrasonic power increases from 20% to 40%, but it significantly increases when the ultrasonic power increases from 40% to 50%. A hole cannot be drilled when the ultrasonic power is at 0%. As illustrated in Figs 7(b) and (c), the chipping size decreases with an increase in the spindle speed and a decrease in the feedrate. The feedrate has a more significant influence on the edge chipping size

15

compared to the ultrasonic power and the spindle speed within the ranges tested.
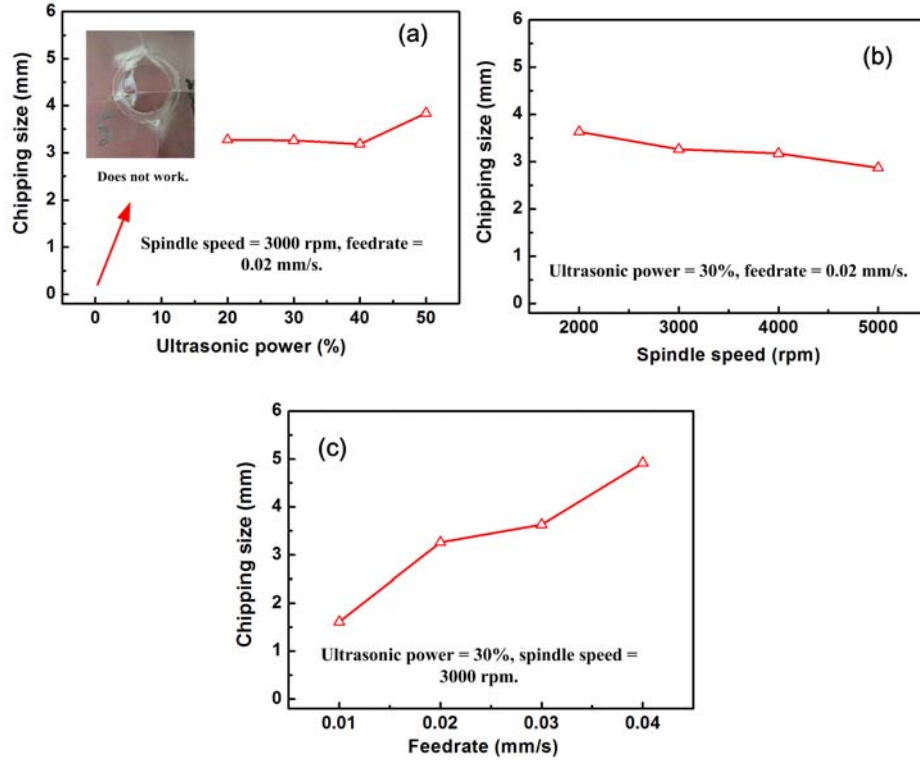

Fig. 7. The effects of the ultrasonic power, the spindle speed and the feedrate on the chipping

size.

Since the edge chipping during the drilling of brittle materials is induced by the fracture failure of machined workpiece, the generating mechanism of edge chipping can be explained by analyzing the stress distribution of the contact area between diamond tool and workpiece. The stress distribution can be calculated as follows

$$\sigma = \frac{4F}{\pi\left(D_o^2 - D_i^2\right)} \tag{2}$$

where F is the axial cutting force (N), D_o and D_i are outer and inner diameter of the tool separately (mm).

Equation (2) shows that the cutting fore has significantly influence on the generation of edge chipping. Jiao et al. reported an investigation on edge chipping in RUM of ceramics, which presented that larger edge chipping is almost always accompanied by a higher cutting force. Therefore, the cutting force features can be used to explain the behaviors of edge chipping, which is shown in below. The changing trends of edge chipping in Fig. 7(b) and (c) are consistent with that of cutting force appeared in Fig. 9(b) and (c). However, the trends appeared in Fig. 7(a) and Fig. 9(a) are inconsistent, which may be because of the change of ultrasonic power. This phenomenon will be discussed in our future work.

3.2 Cutting force

Figure 8 shows a comparison of the cutting force between the RUM process and diamond drilling (RUM without ultrasonic vibration). The machining conditions of Fig. 8 for RUM and diamond drilling are as follows: the ultrasonic power is 0 and 30%, respectively, the spindle speed = 3000 rpm, the feedrate = 0.02 mm/s, the compressed air cooling has a pressure of 40 psi, and the flow rate is 1.5 lpm. Figure 8 shows that the RUM process of optical K9 glass using compressed air as a coolant can significantly reduce the cutting force compared to that induced in diamond drilling.
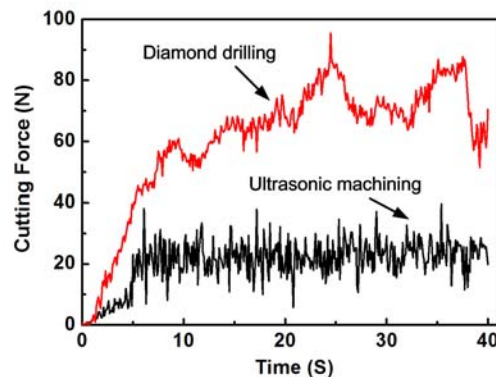
Fig. 8. Comparison of the cutting force between RUM and diamond drilling.

The effects of the ultrasonic power, spindle speed and feedrate on the cutting force are shown in Fig. 9. Figure 9(a) presents the effects of the ultrasonic power on the cutting force. The cutting force decreases when the ultrasonic power increases from 0 to 50%. When the ultrasonic power increases from 0 to 20%, the cutting force decreases from 139.59 N to 49.55 N. With a further increase in the ultrasonic power, the rate of decrease of the cutting force becomes small. The trend of the cutting force versus the increase of the ultrasonic power is consistent with that reported in the paper [24] for the RUM of CFRP using compressed air as a coolant. Figure 9 also shows that, compared to diamond drilling, the RUM of optical K9 glass using compressed air as a coolant can significantly reduce the cutting force.

Figure 9(b) shows the effects of the spindle speed on the cutting force. An increase in the spindle speed reduces the cutting force. The relationship of the feedrate and the cutting force is shown in Figure 9(c). The cutting force increases with an increase in the feedrate. The results of the effects of the spindle speed and feedrate on the cutting force are consistent with those for the RUM of CFRP using cold air as a coolant [24], and the RUM of optical K9 glass using cutting fluid as a coolant [15].
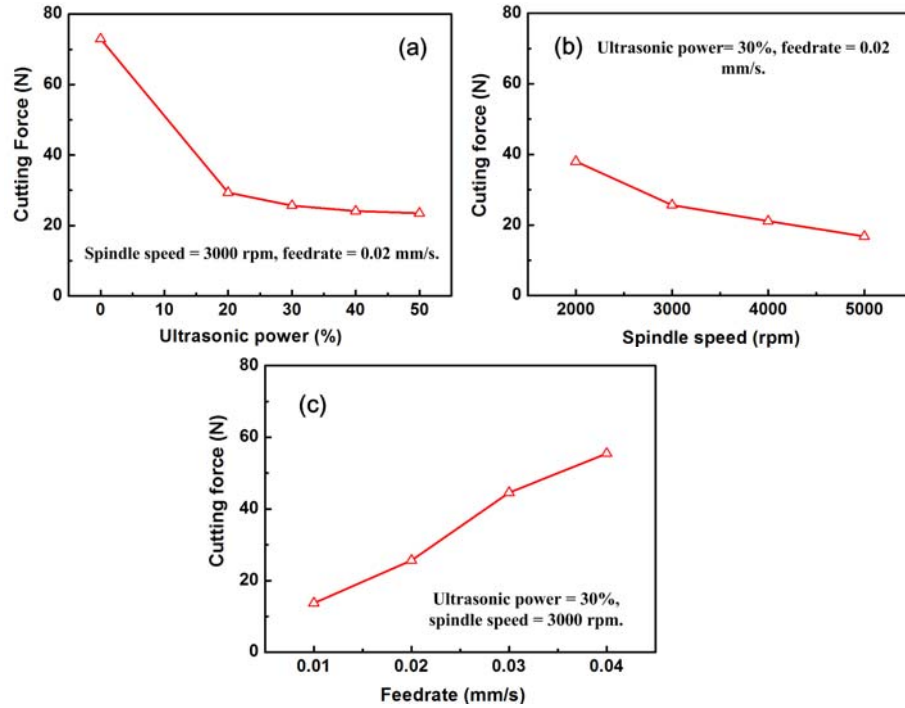
Fig. 9. The effects of the ultrasonic power, the spindle speed and the feedrate on the cutting

force.

3.3 Surface roughness

Figure 10 shows the effects of the input variables on the surface roughness. The relationship between the ultrasonic power and surface roughness is shown in Fig. 10(a). The surface roughness on the machined hole surface increases with an increase in the ultrasonic power. The effects of the spindle speed on the surface roughness, as shown in Fig. 10(b), indicate that increasing the spindle speed can effectively reduce the surface roughness. Figure 10(c) illustrates the relationship between the feedrate and surface

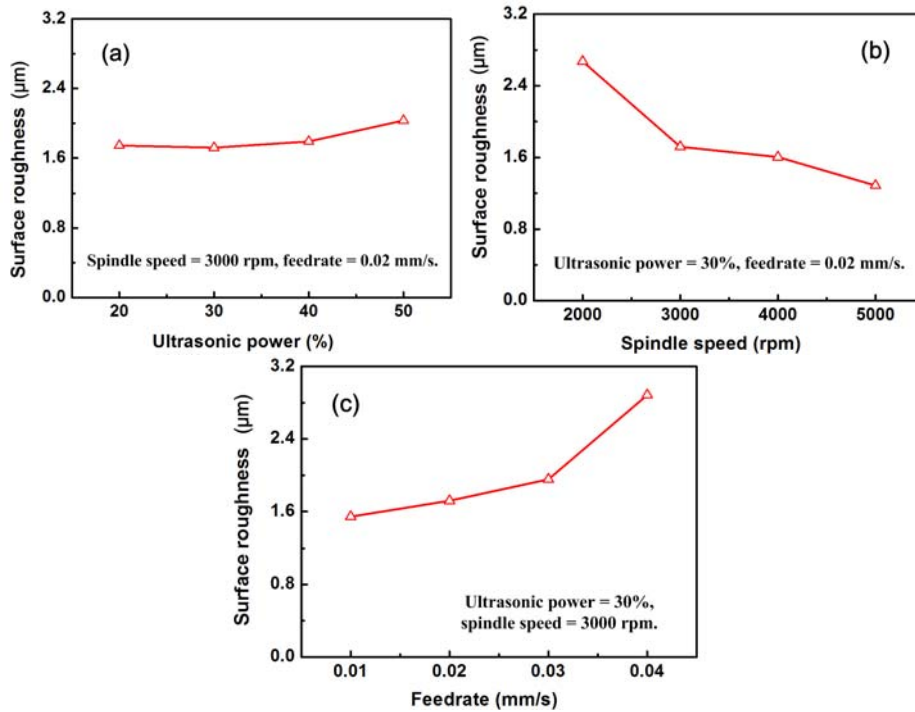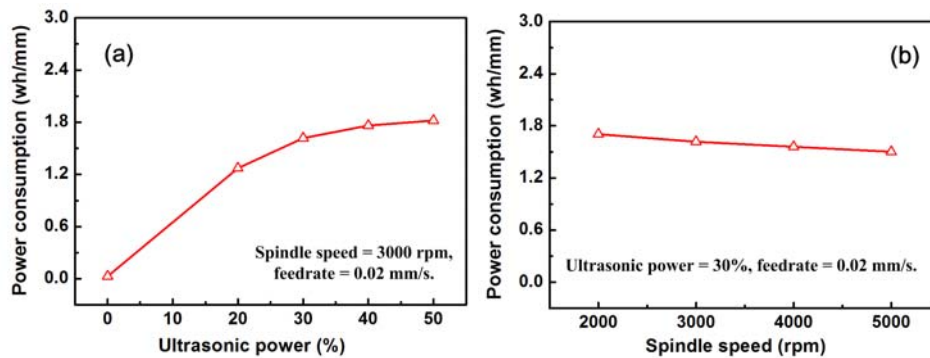roughness. The surface roughness increases as the feedrate increases.

Fig. 10. The effects of the ultrasonic power, the spindle speed and the feedrate on the surface

roughness.

3.4 Ultrasonic power consumption

There is only one paper on the power consumption in the RUM of CFRP using a fluid coolant [27]. The paper reported the results of the effects of the input variables (ultrasonic power, spindle speed, feedrate, and material type) on the power consumption of the entire RUM system and each component (ultrasonic power supply, spindle motor, coolant system, and the air compressor used for feeding the spindle).

The effects of the input variables (ultrasonic power, spindle speed, and feedrate) on the ultrasonic power consumption in the RUM of optical K9 glass using compressed air as a coolant are shown in Fig. 11. Figure 11(a) presents the relationship between ultrasonic power and ultrasonic power consumption. The consumption of ultrasonic power significantly increases when the ultrasonic power increases from 0 to 50%. It is interesting to note that the change of the ultrasonic power consumption with the increase of the ultrasonic power is non-linear, while the relationship between the ultrasonic power and the ultrasonic vibration amplitude is almost linear (as shown in Fig. 3).

The effects of the spindle speed on the ultrasonic power consumption are shown in Fig. 11(b). The ultrasonic power consumption decreases almost linearly as the spindle speed increases. Figure 11(c) presents the effects of the feedrate on the ultrasonic power consumption. It shows that the ultrasonic power consumption decreases as the feedrate increases.
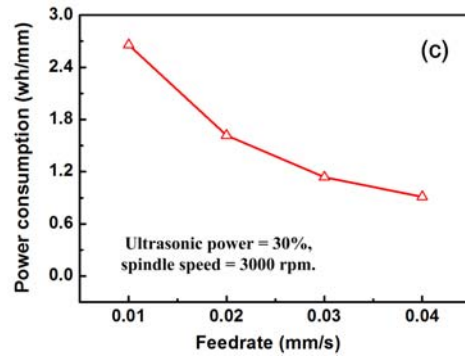
Fig. 11. The effects of the ultrasonic power, the spindle speed and the feedrate on the ultrasonic power consumption.

4. Conclusions

This paper, for the first time, reports an experimental study on the rotary ultrasonic machining (RUM) of optical K9 glass using compressed air as a coolant. The effects of the process parameters (ultrasonic power, spindle speed and feedrate) on the output variables (edge chipping size, cutting force, surface roughness, and power consumption) have been studied. The following conclusions can be drawn from the study:

1. When compressed air is used as coolant, the machining of a hole in an optical K9 glass workpiece can be drilled by RUM but cannot be produced by diamond drilling. Moreover, compared with diamond drilling, RUM has a much lower cutting force.

2. The chipping size decreases slightly with an increase in the ultrasonic power when the ultrasonic power increases from 20% to 40%, but it significantly increases when the ultrasonic power increases from 40% to 50%. The chipping size decreases as the

spindle speed increases and increases as the feedrate increases.

3. As the ultrasonic power or the spindle speed increases, the cutting force decreases. The cutting force increases with an increase in the feedrate.

4. The surface roughness on the machined hole surface increases as the ultrasonic power or the feedrate increases and decreases as the spindle speed increases.

5. The ultrasonic power consumption increases as the ultrasonic power increases and decreases as the spindle speed or the feedrate increases.

References

[1] Gu WB, Yao ZQ and Liang XG. Material removal of optical glass BK7 during single and double scratch tests. Wear 2011; 270(3-4): 241-246.

[2] Fang FZ and Chen LJ. Ultra-Precision Cutting for ZKN7 Glass. Ann CIRP 2000;

49(1): 17-20.

[3] Belkhir N, Bouzid D and Herold V. Surface behavior during abrasive grain action in the glass lapping process. App Surf Sci 2009; 255(18): 7951-7958.

[4] Gu WB, Yao ZQ and Li HL. Investigation of grinding modes in horizontal surface grinding of optical glass BK7. J Mater Process Tech 2011; 211(10): 1629-1636.

[5] Arif M, Rahman M and Yoke San W. Analytical model to determine the critical feed per edge for ductile-brittle transition in milling process of brittle materials. Int J Mach Tool Manuf 2011; 51(3): 170-181.

[6] Park DS, Cho MW, Lee H, et al. Micro-grooving of glass using micro-abrasive jet machining. J Mater Process Tech 2004; 146(2): 234-240.

[7] Matsumura T, Muramatsu T and Fueki S. Abrasive water jet machining of glass with stagnation effect. Ann CIRP 2011; 60(1): 355-358.

[8] Stephenson DJ, Sun X and Zervos C. A study on ELID ultra precision grinding of optical glass with acoustic emission. Int J Mach Tool Manuf 2006; 46(10): 1053-1063.

[9] Zhang CL, Feng PF and Zhang JF. Ultrasonic vibration-assisted scratch-induced characteristics of C-plane sapphire with a spherical indenter. Int J Mach Tool Manuf 2013; 64(1): 38-48.

[10] Pei ZJ, Prabhakar D, Ferreira PM, et al. Mechanistic approach to the prediction of material removal rates in rotary ultrasonic machining. Journal of Engineering for Industry 1995; 117(2): 142-151.

[11] Hu P, Zhang JM, Pei ZJ, et al. Modeling of material removal rate in rotary ultrasonic machining: designed experiments. J Mater Process Tech 2002; 129(1-3): 339-344.

[12] Li ZC, Jiao Y, Deines TW, et al. Rotary ultrasonic machining of ceramic matrix composites: feasibility study and designed experiments. Int J Mach Tool Manuf 2005; 45(12-13): 1402-1411.

[13] Cong WL, Feng Q, Pei ZJ, et al. Edge chipping in rotary ultrasonic machining of silicon. Int J Manuf Res 2012; 7(3): 311-329.

[14] Gong H, Fang FZ and Hu XT. Kinematic view of tool life in rotary ultrasonic side milling of hard and brittle materials. Int J Mach Tool Manuf 2010; 50(3): 303-307.

[15] Zhang CL, Feng PF, Zhang JF, et al. Investigation into the rotary ultrasonic face milling of K9 glass with mechanism study of material removal. Int J Manuf Tech Manag 2012; 25(4): 248-266.

[16] Shokrani A, Dhokia V and Newman SY. Environmentally conscious machining of difficult-to-machine materials with regard to cutting fluids. Int J Mach Tool Manuf

2012; 57(1): 83-101.

[17] Sharma VS, Dogra M and Suri NM. Cooling techniques for improved productivity in turning. Int J Mach Tool Manuf 2009; 49(6): 435-453.

[18] Sreejith PS and Ngoi BKA. Dry machining: machining of the future. J Mater Process Tech 2000; 101(1-3): 287-291.

[19] Choi HZ, Lee SW and Jeong HD. A comparison of the cooling effects of compressed cold air and coolant for cylindrical grinding with a CBN wheel. J Mater Process Tech 2001; 111(1-3): 265-268.

[20] Su Y, He N, Li L, et al. Refrigerated cooling air cutting of difficult-to-cut materials. Int J Mach Tool Manuf 2007; 47(6): 927-933.

[21] Yuan SM, Yan LT, Liu WD, et al. Effects of cooling air temperature on cryogenic machining of Ti–6Al–4V alloy. J Mater Process Tech 2011; 211(3): 356-362.

[22] Nguyen T and Zhang LC. An assessment of the applicability of cold air and oil mist in surface grinding. J Mater Process Tech 2003; 140(1-3): 224-230.

[23] Cong WL, Pei ZJ, Deines TW, et al. Rotary ultrasonic machining of CFRP using cold air as coolant: feasible regions. J Reinf Plastics Comp 2011; 30(10): 899 - 906.

[24] Cong WL, Feng Q, Pei ZJ, et al. Rotary ultrasonic machining of carbon fiber

reinforced plastic composites: using cutting fluid vs. cold air as coolant. J Comp Mater 2012; 46(14): 1745-1753.

[25] Lv DX, Wang HX, Tang YJ, et al. Surface observations and material removal mechanisms in rotary ultrasonic machining of brittle material. Proc Inst Mech Eng, Part B: J Eng Manuf 2012; 226(9): 1479-1488.

[26] Cong WL, Pei ZJ, Mohanty N, et al. Vibration amplitude in rotary ultrasonic machining: a novel measurement method and effects of process variables. J Manuf Sci Eng 2011; 133(3): 034501.

[27] Cong WL, Pei ZJ, Deines TW, et al. Rotary ultrasonic machining of CFRP composites: a study on power consumption. Ultrasonics 2012; 52(8): 1030-1037.